

## References

- <sup>1</sup>Chivens, D.R. and Nelson, H.D., "The Natural Frequencies and Critical Speeds of a Rotating, Flexible Shaft-Disk System," *Journal of Engineering for Industry*, Vol. 97, Ser. B, Aug. 1975, pp. 881-886.
- <sup>2</sup>Klompas, N., "Theory of Rotor Dynamics with Coupling of Disk and Blade Flexibility and Support Structure Asymmetry," *ASME Gas Turbine Conference and Products Show*, ASME Paper 74-GT-159, Zurich, Switzerland, March 30-April 4, 1974.
- <sup>3</sup>Vigneron, F.R., "Comment on 'Mathematical Modeling of Spinning Elastic Bodies for Modal Analysis,'" *AIAA Journal*, Vol. 13, Jan. 1975, pp. 126-127.
- <sup>4</sup>Meirovitch, L., "A Stationarity Principle for the Eigenvalue Problem for Rotating Structures," *AIAA Journal*, Vol. 14, Oct. 1976, pp. 1387-1394.
- <sup>5</sup>Brown, D.P. and Schlack, A.L., Jr., "Stability of a Spinning Body Containing an Elastic Membrane via Liapunov's Direct Method," *AIAA Journal*, Vol. 10, Oct. 1972, pp. 1286-1290.
- <sup>6</sup>Wilgen, F.J., "The Effect of Appendage Flexibility on Shaft Whirl Stability," Ph.D. Dissertation, Dept. of Engineering Mechanics, Univ. of Wisconsin, Madison, Wisc., 1977.
- <sup>7</sup>Colin, A.D., "Modal Analysis for Liapunov Stability of Rotating Elastic Bodies," Ph.D. Dissertation, Engineering-Aeronautical, Univ. of California, Los Angeles, Calif., 1973.
- <sup>8</sup>Likins, P.W., Barbera, F.J., and Baddeley, V., "Mathematical Modeling of Spinning Elastic Bodies for Modal Analysis," *AIAA Journal*, Vol. 11, Sept. 1973, pp. 1251-1258.

## A Paradoxical Case in a Stability Analysis

R. Parnes\*

Tel-Aviv University, Ramat-Aviv, Israel

IN analyzing elastic systems subjected to compressive loads, it is generally accepted that the load at which instability occurs decreases as the member increases in length. In the model investigated below, the opposite is found to be true. Aside from its academic interest, the implications of the behavior of the given model may be of some significance, for example, in the design of prostheses.

Consider the model shown in Fig. 1a, where  $EI$  and  $E'I'$   $= \alpha^2 EI$  are the flexural rigidities of members  $AB$  and  $BC$ , respectively, and where  $L$  and  $cL$  are the respective lengths. From stability theory, one might conclude that the axial load  $P$  at which instability occurs decreases for all increasing values of the parameter  $c > 0$ . However, as is shown below, such behavior exists only within a range  $c_0 < c$ , where  $c_0$  is a constant dependent on  $\alpha$ . Paradoxically, for values  $c < c_0$ , increasing the length of the member *increases* the buckling load.

We first consider the simpler case where member  $BC$  is infinitely rigid i.e.,  $E'I' \rightarrow \infty$  or  $\alpha \rightarrow \infty$ . The resulting neutral equilibrium position in the deformed state is as shown in Fig. 1b, where  $\Delta = v(L)$  is a small displacement.

The corresponding eigenvalue problem then consists of the equilibrium equation

$$\frac{d^2 v(x)}{dx^2} + \beta^2 v(x) = \beta^2 \Delta \left[ 1 + \frac{1}{c} - \frac{x}{cL} \right] \quad (1)$$

and the boundary conditions

$$v(0) = \frac{dv(0)}{dx} = 0, \quad v(L) = \Delta \quad (2)$$

Received May 27, 1977.

Index categories: Structural Design; Structural Stability.

\*Associate Professor, Department of Solid Mechanics, Materials and Structures, School of Engineering.

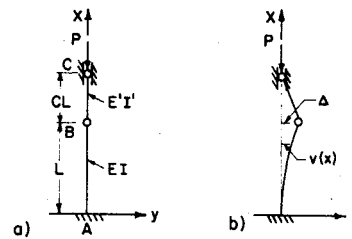


Fig. 1 Geometry of problem.

where

$$\beta^2 = P/EI \quad (3)$$

Solutions of this boundary-value problem lead to eigenvalues that are the roots of the equation

$$f(\beta L) \equiv \tan \beta L - (1+c)\beta L = 0 \quad (4)$$

It is recognized that, when  $c=0$ , we recover the known transcendental equation for a member fixed at one end and hinged at the other, while as  $c \rightarrow \infty$  we obtain the equation  $\cos \beta L = 0$ , which corresponds to a cantilevered-free end member subject to an axial load, where the smallest load of instability is the classical value<sup>1</sup>

$$P_E = \pi^2 EI / 4L^2 \quad (5)$$

For the problem at hand, the loads causing instability, obtained from Eq. (4), are plotted in nondimensional form  $P/P_E$  as a function of the parameter  $c$  (solid line) in Fig. 2. It is noted that, as  $c \rightarrow 0$ , the value of  $P$  approaches zero, whereas for all  $c \rightarrow \infty$  the value  $P \rightarrow P_E$  asymptotically. Thus, for increasing lengths of  $cL$ , the load  $P$  required to cause instability actually increases; the value  $c_0$ , as previously defined, is infinite.

The usual behavior of small values of  $c$  now can be examined more closely. It is evident that, when  $c=0$  identically, we obtain from Eq. (4) the classical value<sup>1</sup>

$$P = [\pi^2 EI / (0.7L)^2] > P_E \quad (6)$$

although Fig. 2 indicates values approaching zero.

The apparent discrepancy may be explained by considering the graph of Fig. 3, showing the roots of Eq. (4). It is realized immediately that, for  $c=0$ , the relevant root is given by point A, whereas for any  $c > 0$  the relevant root is represented by the generic point B, which lies on a different branch. As  $c \rightarrow \infty$ , again  $\beta L \rightarrow \pi/2$ , and thus  $P/P_E \rightarrow 1$ , as shown in Fig. 2.

In the preceding analysis, member  $BC$  was assumed rigid for mathematical simplicity. If we return to the problem where member  $BC$  has a finite flexural rigidity  $E'I' = \alpha^2 EI$ , we obtain, in lieu of Eq. (4), the uncoupled equation

$$\sin(\beta cL/\alpha) [\tan \beta L - (1+c)\beta L] = 0 \quad (7)$$

The roots of this equation are clearly the same as those obtained previously from  $f(\beta L) = 0$ , with additional roots from the equation

$$\sin(\beta cL/\alpha) = 0 \quad (8)$$

which correspond to the instability of member  $BC$  considered as a pin-connected member. The actual load causing instability is then the smaller of the two roots given by Eq. (4) or (8), depending on the relative geometry and stiffnesses, i.e., on the parameters  $c$  and  $\alpha$ . The nondimensional instability loads  $P/P_E$  are plotted as a function of  $c$  in Fig. 2, where the dashed lines, representing the loads corresponding to the roots of Eq. (8) for the family of curves of  $\alpha$ , are given by

$$P/P_E = 4\alpha^2 / c^2 \quad (9)$$

Fig. 2 Buckling load vs length.

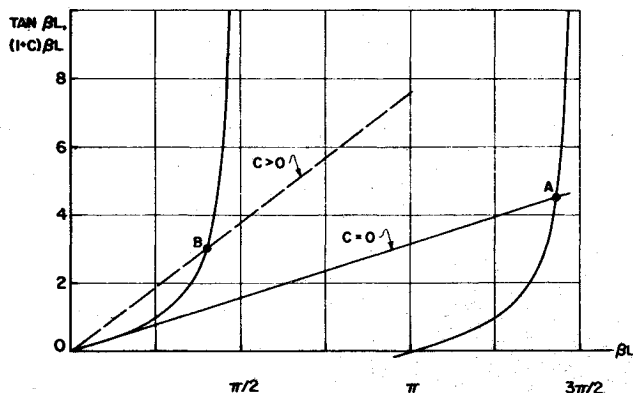
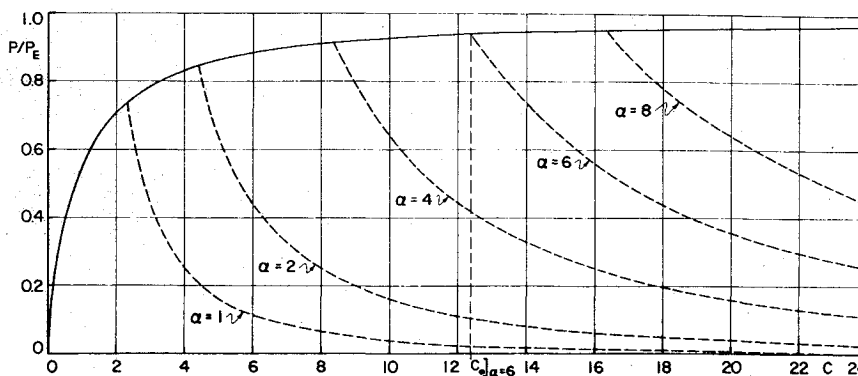


Fig. 3 Roots of Eq. (4).

Thus it is seen again that, for finite values of  $\alpha$ , greater loads are required for instability for increasing lengths in the range  $c < c_0$ , where  $c_0 = c_0(\alpha)$ . The solid lines represent the instability caused by bending of member  $AB$ . For values  $c_0 < c$ , instability occurs due to buckling of member  $BC$ , and thus we arrive again at the classical case where a system of increasing length buckles under smaller loads.

The preceding results should be taken into account in the design of members conforming to a system represented by Fig. 1, where it is seen that increasing the value of  $c$  within the range  $0 < c \leq c_0$  actually may improve design in the context of stability criteria.

### References

- <sup>1</sup>Timoshenko, S. and Gere, J., *Theory of Elastic Stability*, McGraw-Hill, New York, 1961.

## Technical Comments

### Comment on "Effective Thermal Property Improves Phase Change Paint Data"

Alexander H. Flax\*

Institute for Defense Analyses, Arlington, Va.

**D**RUMMOND et al.<sup>1</sup> have found "effective" steady-state thermophysical parameters for materials specimens representative of thin-wing models based on numerical analysis employing experimentally determined thermophysical material properties. For homogeneous materials, their data indicate that a single "effective" parameter that is a function of surface temperature only and is independent of heating rate describes the results; For nonhomogeneous samples the "effective" parameter depends both on surface temperature and on heating rate. In either case, the "effective" parameter values are different from those that would be deduced from the temperature-dependent properties of the materials measured in steady-state heat conduction tests. The purpose of this Comment is to show that these results are consequences of the basic equations of transient heat conduction in solids and hence applicable to a much broader range of temperature, materials, and geometric configurations than represented in the numerical calculations.

Received May 26, 1977; revision received July 1, 1977.

Index category: Thermal Surface Properties.

\*President, Fellow AIAA.

Consider the three-dimensional transient heat conduction equation in which the thermal conductivity  $k$ , and the heat capacity  $c$ , are functions of temperature  $T$ :

$$\frac{\partial}{\partial x} \left[ k(T) \frac{\partial T}{\partial x} \right] + \frac{\partial}{\partial y} \left[ k(T) \frac{\partial T}{\partial y} \right] + \frac{\partial}{\partial z} \left[ k(T) \frac{\partial T}{\partial z} \right] = \rho c(T) \frac{\partial T}{\partial t} \quad (1)$$

where  $\rho$  is the density.

The boundary condition for surface heat transfer given over the surface is

$$-k(T_s) \left( \frac{\partial T}{\partial n} \right)_s = Q \quad (2)$$

where  $s$  denotes surface,  $\partial T / \partial n$  is the normal derivative, and  $Q$  is the heating rate, constant over the surface.

The boundary condition (2) and differential equation (1) may be normalized with respect to heating rate by dividing through by  $Q$  and  $Q^2$ , respectively. Making the substitutions

$$\xi = Qx \quad \eta = Qy \quad \zeta = Qz \quad \tau = Q^2 t$$

leads to the equations

$$\frac{\partial}{\partial \xi} \left[ k(T) \frac{\partial T}{\partial \xi} \right] + \frac{\partial}{\partial \eta} \left[ k(T) \frac{\partial T}{\partial \eta} \right] + \frac{\partial}{\partial \zeta} \left[ k(T) \frac{\partial T}{\partial \zeta} \right] = \rho c(T) \frac{\partial T}{\partial \tau} \quad (3)$$